

Power Optimizations in MTJ-based Neural Networks through Stochastic Computing

Ankit Mondal and Ankur Srivastava

Department of Electrical and Computer Engineering, University of Maryland, College Park, MD 20783, USA
Email: {amondal2, ankurs}@umd.edu

Abstract—Artificial Neural Networks (ANNs) have found widespread applications in tasks such as pattern recognition and image classification. However, hardware implementations of ANNs using conventional binary arithmetic units are computationally expensive, energy-intensive and have large area overheads. Stochastic Computing (SC) is an emerging paradigm which replaces these conventional units with simple logic circuits and is particularly suitable for fault-tolerant applications. Spintronic devices, such as Magnetic Tunnel Junctions (MTJs), are capable of replacing CMOS in memory and logic circuits. In this work, we propose an energy-efficient use of MTJs, which exhibit probabilistic switching behavior, as Stochastic Number Generators (SNGs), which forms the basis of our NN implementation in the SC domain. Further, error resilient target applications of NNs allow us to introduce Approximate Computing, a framework wherein accuracy of computations is traded-off for substantial reductions in power consumption. We propose approximating the synaptic weights in our MTJ-based NN implementation, in ways brought about by properties of our MTJ-SNG, to achieve energy-efficiency. We design an algorithm that can perform such approximations within a given error tolerance in a single-layer NN in an optimal way owing to the convexity of the problem formulation. We then use this algorithm and develop a heuristic approach for approximating multi-layer NNs. To give a perspective of the effectiveness of our approach, a 43% reduction in power consumption was obtained with less than 1% accuracy loss on a standard classification problem, with 26% being brought about by the proposed algorithm.

I. INTRODUCTION

The capability of the human brain to learn and solve complex problems have inspired advancements in areas of neuroscience, artificial intelligence and machine learning. Decades of research in Artificial Neural Networks (ANNs), despite our limited understanding of biological Neural Networks (NNs), have shown promising results in applications such as pattern recognition and image classification [1]. However, a typical ANN can have thousands of neurons and synapses, making their hardware implementation both computation and memory-intensive. This has prompted the development of optimization techniques at different levels of these complex networks to achieve energy efficiency [2] [3].

Approximate Computing is an emerging concept which involves the computation of imprecise results in order to achieve significant reductions in power consumption [4]. The inherent error-resilience of Recognition, Mining and Synthesis applications make them a perfect candidate for such trade-off between the quality of results and the energy requirements. A similar paradigm is Stochastic Computing (SC) which concerns the use of low-cost logic gates, instead of binary arithmetic units, for computations [5]. In SC, data, which are interpreted as probabilities and called Stochastic Numbers (SNs), are represented in the form of bit streams of 0s and 1s and generated by circuits called Stochastic Number Generators (SNGs). SC has been shown to be significantly energy-efficient when compared to conventional methods.

Magnetic Tunnel Junction (MTJ) is one of several emerging spintronic devices. Apart from non-volatility, its high integration density, scalability and CMOS compatibility make it a suitable candidate for replacing CMOS in future memory devices [6]. The Spin-Transfer Torque RAM, which is based on MTJs, has

been explored as a memory device. While a lot of research has focused on reducing its critical switching current density to lower the write energy, attempts have been made to exploit the probabilistic switching characteristics of MTJs to use them as SNGs, such as in [7], that could produce bit streams representing any fraction between 0 and 1.

This paper integrates SC based on MTJs into ANNs and explores the different ways of achieving energy efficiency at both the device level and the network level, in the latter through approximations. Our contributions are summarized as follows:

- We outline the characteristics of an MTJ with regard to switching time and energy, develop a low-power MTJ-SNG by exploiting the properties of SC, and compare it with the baseline.
- We propose the use of our MTJ-SNG as an architectural construct for ANNs in the SC domain. We develop an optimization algorithm, that approximates the synaptic weights in a 1-layer NN, for achieving energy-efficiency by sacrificing little accuracy.
- This algorithm is then extended to a multi-layer NN by heuristically breaking down the entire problem into separate problems for each layer and solving them optimally.

II. PRELIMINARIES

This section explains the basics of Neural Networks relevant to this paper, their structure and functioning, and mentions prior work similar to ours.

A. Neural Network Architecture

The fundamental units of an NN are *neurons*, which represent non-linear, bounded functions, and *synapses*, which are interconnections between neurons. Each neuron performs a weighted sum of its inputs, which in turn is fed to a non-linear activation function to squash the output to a finite range [1]. The output of a neuron, called the *activation level*, can be expressed as

$$y = f \left(\sum_{i=1}^N w_i x_i + b \right) \quad (1)$$

where N is the no. of inputs to the neuron, w_i is the synaptic weight of the connection from the i^{th} input x_i , b is a bias, and $f()$ is an activation function (such as \tanh or sigmoid). Fig. 1(a) depicts the operations performed by a neuron and 1(b), the behaviour of the \tanh function.

Feedforward networks are the most elementary Neural Networks, in which information flows only in one direction from the input to the output, represented by an acyclic graph. The simplest feedforward network, called a Perceptron, contains just the input and output layers. More popular and useful are the Multi-layer Perceptrons (MLPs) which have one or more layers of neurons, called hidden layers, between the inputs and the outputs (fig. 1(c)).

The most popular technique of training an NN is the *error back-propagation* method, which relates the error or cost function with the weights of all the layers. This kind of a “backward calculation” is used to compute the gradient of the error function

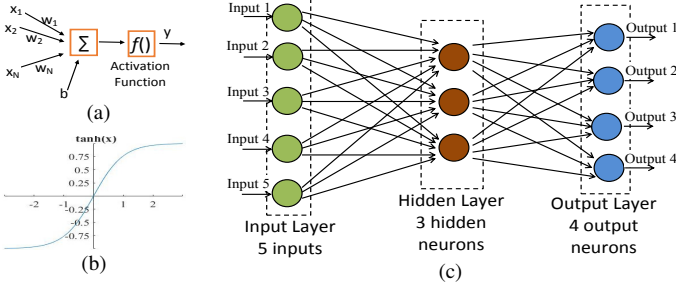


Fig. 1: (a) A neuron. (b)The \tanh function. (c) Schematic of an MLP with one hidden layer.

that is then used to update the weights in the direction in which error goes down the steepest [1]. This is known as gradient descent or the delta rule and is given as

$$\Delta w_i = -\eta \frac{\partial E}{\partial w_i} \quad (2)$$

where η is known as the learning rate and E is the error function.

B. Stochastic Computing

In contrast to conventional arithmetic computing, SC uses bit streams to represent numbers, typically denoted by the probability of '1's in the stream. An SN with value $p \in [0, 1]$ is represented as a sequence of bits, such that if there are n bits in the sequence, out of which k are '1', then $p = \frac{k}{n}$ [5]. This is known as the *unipolar* format. In the *bipolar* format, $p \in [-1, 1]$, and the same bit sequence would now have the value $p = \frac{2k-n}{n}$. For example, the bit stream 0100101000 would be interpreted as 0.3 in the unipolar format and -0.4 in the bipolar format.

In SC, multiplication is performed by an AND gate in the unipolar format [5]. Thus, given 2 stochastic streams X and Y , their product is $\text{AND}(X, Y)$. In the bipolar format, it is given as $\text{XNOR}(X, Y)$. However, it is not possible to perform a precise addition in the SC domain as the sum of 2 SNs might very well lie beyond the range. Only a scaled addition is possible which is achieved through a 2:1 Mux whose Select input is the scaling factor and is also an SN. The scaled additon of A and B , with scaling factor S , would give $Z = A.S + B.(1-S)$ as in fig. 2(a). With $S = 0.5$, one can get $\frac{A+B}{2}$, albeit with a loss of precision. However, most implementations of NNs involve the sum of a large number of numbers and a loss of precision would only result in severe errors at its outputs.

To overcome this issue, Ardkhani et al. [8] introduce the concept of Integral Stochastic Computing (ISC) which allows us to represent numbers beyond the range of conventional SC. In the unipolar format, a real number $s \in [0, m]$ can be expressed as the sum of m numbers $s_1, s_2, \dots, s_m \in [0, 1]$. Each of the s_i s can be represented as stochastic streams and s can be obtained as the bit-wise summation of these m streams as illustrated by an example in fig. 2(b). In general, a number $s \in [0, m]$, when represented as the sum of m SNs, would require $\lceil \log_2 m \rceil + 1$ streams (similar to a binary representation). This concept extends similarly to the bipolar format as well [8].

Multiplication and addition in ISC are performed using binary radix multipliers and adders respectively. Given 2 real numbers $s_1 \in [0, m_1]$ and $s_2 \in [0, m_2]$, their product and sum would have $\lceil \log_2(m_1 m_2) \rceil + 1$ and $\lceil \log_2(m_1 + m_2) \rceil + 1$ bits respectively in

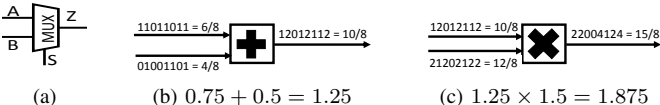


Fig. 2: (a) Scaled addition in SC, (b) Integral SC (ISC) representation ($m = 2$), and (c) Multiplication in ISC ($m_1 = m_2 = 2$)

the ISC domain. Fig. 2(c) gives an example. It is also possible to design a good approximation to non-linear functions, such as \tanh , in ISC using a Finite State Machine [8].

C. Related Work

Several research efforts have been made both towards the efficient implementation of deep neural networks through approximations (as in [3], [9] and [2]) and towards the realization of NN hardware with non-conventional methods of computation. Tarkov [10] proposes using a memristor as a device that stores synaptic weights, thereby obviating the need for a large amount of memory, and develops an algorithm for mapping a weight matrix onto a memristor crossbar. Hu et al. [11] extend this idea by developing a Dot-Product Engine (DPE) for matrix-vector multiplications by taking into account the device and circuit issues. In [8] Ardkhani et al. design an efficient implementation of an NN in the ISC domain. They achieve significant reduction in power consumption at the same rate of misclassification when compared to CMOS implementation. Kim et al. [12] combine the ideas of SC in DNN and energy-accuracy trade-off by removing near-zero weights during the training phase (and later retraining the network), combining the addition and squashing operations and incorporating progressive precision in the SC bit streams. Venkatesan et al. [13] proposed a spintronic-based Stochastic Logic which used the random switching characteristics of a nanomagnet to generate random numbers and MTJs to store them in binary form.

III. MTJ-BASED STOCHASTIC COMPUTING

In this section we shall describe the probabilistic switching characteristics of an MTJ and exploit the properties of Stochastic Numbers to design a low-power optimized MTJ-based SNG and compare it to its non-optimized version. This MTJ-SNG would be the underlying source of approximations in our energy-efficient NN implementation.

A. Characteristics of Magnetic Tunnel Junctions

MTJ is the most popular spintronic device being considered for NVM technologies [6]. An MTJ can exist in one of 2 states depending on the relative magnetizations of its free and fixed layers – Parallel (P, logic 0) or Anti-Parallel (AP, logic 1). MTJs exhibit spin-torque transfer effects – spin polarized current, when passed through an MTJ, can switch the magnetization of its free layer. Depending on the switching pulse width, MTJs exhibit 3 switching modes – Precessional (< 3 ns), Dynamic Reversal (3 to 10 ns) and Thermal Activation (> 10 ns) [14]. Since we desire a high-speed SNG, we operate in the Precessional mode (high currents leading to switching times of the order of few ns), where the probability density function of the switching time is given as¹

$$P(t_p) \propto e^{-\Delta \sin^2 \phi} (J - J_{c0}) \sin^2 \phi \quad (3)$$

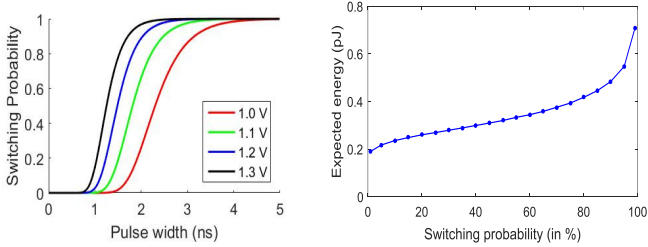
with $\Delta = \frac{H_K M_s V}{2k_B T}$ and $\phi = \frac{\pi}{2} e^{-\frac{\eta \mu_B}{e M_s t_F} (J - J_{c0}) t_p}$

We have simulated the behavior of an MTJ with in-plane magnetic anisotropy using an MTJ Spice Model² [6]. The values of J_{c0} obtained were 7.55MA/cm^2 for P \rightarrow AP switching and 4.10MA/cm^2 for AP \rightarrow P switching and of Δ was 47.5.

Given a pulse of width T_p , the probability that switching takes place within T_p is

¹ H_K is the shape anisotropy field, M_s is the saturation magnetization, V is the volume of the free layer, k_B is the Boltzmann constant, T is the temperature, J is the current density, J_{c0} is the critical current density, η is the spin transfer efficiency, t_F is the thickness of the free layer and t_p is the pulse duration.

² The parameters used were - cell dimension $20 \times 58 \text{nm}^2$, $t_F = 2.5 \text{nm}$, $M_s = 1222 \text{emu/cc}$, α (damping constant) = 6.82×10^{-3} , $\eta = 0.85$, RA product = $5 \Omega \mu\text{m}^2$, $T = 300 \text{K}$.



(a) Probability v/s pulse width (b) Energy v/s probability, $V_{bias} = 1.2V$

Fig. 3: MTJ switching characteristics for $AP \rightarrow P$ transition.

$$P_{sw}(T_p) = \int_0^{T_p} P(t)dt \quad (4)$$

where $P_{sw}(t)$ is the switching probability (the cumulative distribution function), and the expected time at which switching takes place (given it does) with pulse width T_p , is expressed as

$$E(t_{sw}) = \int_0^{T_p} tP(t)dt \quad (5)$$

Let I_{AP} and I_P denote the currents in the AP and P state respectively. The expected energy consumed in such a scenario, for $AP \rightarrow P$ switching, is

$$E_{sw}^{AP \rightarrow P} = V(I_{AP}E(t_{sw}) + I_P(T_p - E(t_{sw}))) \quad (6)$$

whereas the energy spent in the case where switching does not take place is

$$E_{nsw}^{AP \rightarrow P} = VI_{AP}T_p \quad (7)$$

Thus the overall expected energy consumed is given as

$$E = P_{sw}(T_p)E_{sw}^{AP \rightarrow P} + (1 - P_{sw}(T_p))E_{nsw}^{AP \rightarrow P} \quad (8)$$

B. MTJ as a Stochastic Number Generator

An MTJ can be used as an SNG by exploiting the probabilistic nature of its switching. Given a voltage pulse, the probability of switching can be decided by controlling the pulse width. The probabilities for $AP \rightarrow P$ switching, for different voltage bias, are shown in fig 3(a). For each bit generated by the MTJ representing a stochastic number $p \in [0, 1]$, one would typically do the following iteratively:

- Reset to 0 with 100% probability (not required if state didn't change in the previous iteration)
- Write 1 with probability p , and
- Read the value stored in the MTJ (which would be 1 with probability p and 0 with probability $1 - p$).

Repeating this procedure n times would give us a sequence of n bits, out of which $p.n$ are expected to be 1, thereby representing the SN p . However, the expected energy required for switching $P \rightarrow AP$ (logic 0 → 1) with 99.9% probability is $0.46pJ$; whereas that for $AP \rightarrow P$ (logic 1 → 0) is $0.93pJ$ with 1.2V. We thus choose the AP state (logic 1) to be the reset state, and switch to the P state (logic 0) with some probability (because resetting $P \rightarrow AP$ would require lesser energy than $AP \rightarrow P$). This means that switching $AP \rightarrow P$ with probability x will generate bit streams where the probability of finding '1's is $1 - x$. Hence, to represent the stochastic number p , we shall write 0 with probability $1 - p$.

The expected energy consumption was found to be minimum for a voltage bias of about 1.2V. We thus use this for writing to the MTJ. Plotted in fig. 3(b) is the trade-off between energy and switching probability. Resetting the MTJ requires a pulse width of $4.33ns$, and switching to '0' with 99.9% probability requires $3.40ns$. Reading the value stored in the MTJ using a sense amplifier can be done with a bias of $-0.1V$ for $2ns$. Thus, the total time necessary for generating one bit of the SN is (a maximum of) $9.73ns$.

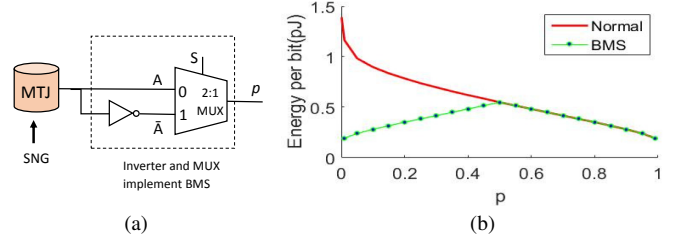


Fig. 4: (a) Circuit of the BMS. (b) Energy per bit v/s Value of SN p

C. Proposed Biased MTJ-SNG

We make a slight modification to the overall procedure of generating the bits of the SN. As seen earlier, generating an SN with value p using our MTJ implies that the probability of switching from $AP \rightarrow P$ (which is the same as writing 0) has to be $1 - p$. If p is closer to 0, then $1 - p$ is closer to 1; which implies more time, and hence more energy, has to be spent in writing '0' to the MTJ, as compared to the case where we had to generate an SN with value $1 - p$. To prevent this characteristic from making the SNG energy-intensive, we choose to generate $1 - p$ whenever $p < 0.5$ (but generate p if $p \geq 0.5$). In other words, whenever $p < 0.5$, instead of switching $AP \rightarrow P$ with probability $(1 - p)$ (which is ≥ 0.5), we switch with probability p . Now all we would need to do is to invert the bits output from this Biased MTJ-SNG (**BMS**, the name being derived from the biased nature of the data produced by the MTJ-SNG) so that we get back the SN p . Therefore, we generate either p or $1 - p$, whichever is larger, and use a 2:1 multiplexer to choose between the generated SN and its inverse as shown in fig. 4(a). The inputs to the Select pin of the multiplexer can be derived from the most significant bit of the binary number that is being converted to a stochastic number [5]. As an example, if $p = 0.7$, the MTJ-SNG will generate p itself and S will be 0 to output $A = 0.7$. On the other hand, if $p = 0.3$, the MTJ will generate $(1 - p) (= 0.7)$ and S will be 1 to output $\bar{A} = 0.3$.

The energy required to generate one bit from the MTJ-SNG is plotted in fig. 4(b) as a function of p for both the cases - without any modification (Normal), and with BMS in place (including the overheads due to the mux and inverter). The symmetry of the plot with BMS (dotted line) comes from generating the larger of p and $1 - p$. Table I compares the 2 MTJ-SNGs. Since the BMS requires us to generate SNs only greater than or equal to 0.5, the maximum write duration reduces from $3.40ns$ to $1.49ns$ (the latter corresponds to the pulse width giving 50% switching probability), thereby decreasing the total time. The average energy and power have been calculated considering a uniform distribution of p over the range $[0, 1]$; BMS brings about a reduction by 42% and 23% respectively (without introducing any approximation or error in the SN being generated.)

TABLE I: Comparison of Normal and Biased MTJ-SNG

MTJ-SNG	Time(ns)	Avg. Energy (pJ)	Avg. Power (μW)
Normal	9.73	0.59	80
BMS	7.82	0.34	62

IV. ENERGY EFFICIENT MTJ-BASED NN IMPLEMENTATION

Stochastic circuits have gained popularity in low-cost implementation of NNs [8] [12]. We propose using MTJs as a hardware component for realizing NNs in the SC domain by exploiting their probabilistic switching nature to generate SNs representing inputs and synaptic weights. The error-resilient nature of NN applications motivate us to approximate the weights, effectively designing approximate multipliers, and thereby gaining energy efficiency. In this section, we develop an algorithm that, given a trained network, the training dataset and an error tolerance, adjusts the weights in the best possible way

in the solution space, while remaining within the error constraint at all times.

A. NN implementation in the SC/ISC domain

Here we describe how the operations of a neuron would be performed in the ISC domain (refer to section II-B). We know that the activation level of a neuron is given as

$$t = f(a) = f \left(\sum_{i=1}^N \tilde{w}_i \tilde{x}_i \right) \quad (9)$$

where f is the activation function operating on a , the weighted sum of inputs. Several types activation functions can be used in an NN. We go for the \tanh function because it is non-linear and has a bipolar output. In eqn. (9), the \tilde{x}_i s (inputs) are assumed to be in the range $[0, 1]$ (and are typically so) and \tilde{w}_i s (weights) are generally in $[-M, M]$ with $M > 1$. The latter can be represented in the ISC domain with $\lceil \log_2 M \rceil + 1$ stochastic streams; however, this would need those many SNGs, leading to high energy consumption. Therefore, we have to scale them down to the range $[0, 1]$ or $[-1, 1]$ to be able to use only 1 stream. Since the ISC implementation of the \tanh function using FSM is in bipolar format, we go for the interval $[-1, 1]$. Further, it is necessary to have a single format throughout, thereby requiring us to scale down the inputs to the range $[-1, 1]$. So the weighted sum would now be written as

$$a = \frac{M}{2} \left(\sum_{i=1}^N w_i x_i + \sum_{i=1}^N w_i \right) \quad (10)$$

where $x_i, w_i \in [-1, 1] \forall i$. Fig. 5(a) illustrates the operations of a neuron in the ISC domain, implementing eqns. (9) and (10). Several such neurons in parallel would form a layer as in fig. 1(c), and multiple layers connected in series would make up the entire network. Note that the output of the \tanh is a single stochastic stream in the bipolar format.

B. Problem Formulation

As can be seen from fig. 4(b), the generation of SNs (from the proposed BMS) that are closer to 0 or 1 require less energy as compared to those that are closer to 0.5. In the bipolar format of SC, this would imply low energy requirement for numbers closer to 1 or -1 than to 0. This property of the BMS forms the basis of achieving energy-efficiency through approximations that tend to shift the weights “farther from” 0 towards 1 or -1 , whichever is closer. We therefore aim to bring the weights of the network as close to 1 or -1 as possible while ensuring that output errors are within a tolerance level for all the training inputs. We investigate both single-layer and multiple-layer NNs.

C. Optimizing a 1-layer NN

For a single layer network, we illustrate how to formulate the approximation as a convex optimization problem. Convexity of the feasible region of such a problem implies that any local minimum in that region is also the global minimum, ensuring that the optimum value of the objective function is always achieved. Further, non-convex optimization problems are more complicated to solve.

The objective of our formulation is to minimize the separation

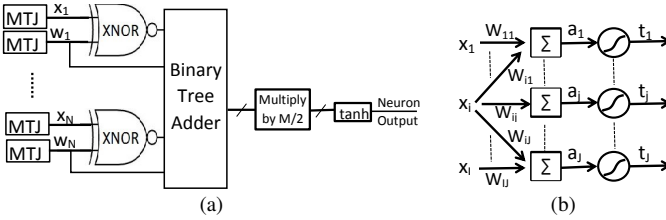


Fig. 5: (a) Neuron implementation in ISC (b) Schematic of 1-layer NN

of the weights from 1 or -1 (whichever is closer). Since the weights are independent of each other, the objective function can be expressed as the sum of the “distance” of the weights from 1 or -1 . One way of specifying an error tolerance at the output layer is to measure the deviation of the output neurons from their actual values (the values obtained from the trained network) and restrict all of them to within some threshold. Such a constraint should be also be applicable for all input vectors used in the optimization.

However, the \tanh function (which provides the neuron output) is not only non-linear but also non-convex. Thus, neither neuron activation levels nor the errors in them can be directly incorporated in the convex formulation. But the input to this activation function is affine (hence convex) because it is a weighted sum of inputs. We therefore need to translate the output errors to errors in inputs of \tanh . Given a limit to the deviation in neuron output, we pre-compute the upper and lower limits of the weighted sum input using the \tanh^{-1} function and force it to remain within these limits.

Fig. 5(b) illustrates a 1-layer network having I inputs and J outputs and table II lists the notations. In addition, the presence of $\hat{\cdot}$ (hat) symbol indicates that the quantity is the original value obtained from the trained network, and hence is a constant in the problem; whereas its absence denotes a variable.

TABLE II: Notations for problem formulation of 1-layer NN

Name	Meaning	Type	Dimension
W	The output layer weight matrix	Matrix	$I \times J$
\hat{x}^r	The r^{th} training sample (input vector)	Vector	I
M	The scaling factor for W	Scalar	1
a^r	The r^{th} weighted sums (output layer)	Vector	J
t^r	The r^{th} activation levels (output layer)	Vector	J

The Optimization Procedure: The procedure for approximating weights in a 1-layer NN is shown below. It takes a trained network and an error threshold ϕ as inputs, and minimizes the “sum of distances” using D samples of the training dataset. Line 2 computes the maximum and minimum values that the weighted sum inputs of the \tanh function can take. Here t_j^r denotes the output of the j^{th} neuron for the r^{th} training input, and u_j^r & v_j^r are the corresponding limits. The objective function (line 3) to be minimized is the sum of distances of the weights from 1 or -1 . W' in line 5 stores how

Weight Approximation for a single-layer NN

- 1: **procedure** OPTIMWEIGHTS($I, J, \hat{W}, \hat{x}, \hat{t}, M, \phi$)
 - 2: The constraint on the neuron outputs are $|t_j^r - \hat{t}_j^r| \leq \phi$. Compute the upper and lower limits of all weighted sums as
 $u_j^r = \tanh^{-1}(\hat{t}_j^r + \phi)$ and
 $v_j^r = \tanh^{-1}(\hat{t}_j^r - \phi)$ respectively $\forall r = 1 \dots D, j = 1 \dots J$
 - 3: Solve the optimization problem:
 $\underset{W}{\text{minimize}} \quad W_{sod} = \sum_{i=1}^I \sum_{j=1}^J W'_{ij}$
subject to the following constraints (lines 4 to 7):
 - 4: Restrict the weights to their original range.
if $(\hat{W}_{ij} \geq 0)$ **then** $0 \leq W_{ij} \leq 1$
else $-1 \leq W_{ij} \leq 0$ $\forall i = 1 \dots I, j = 1 \dots J$
 - 5: See how far the weights are from 1 or -1 , whichever is closer
 $W'_{ij} = \begin{cases} 1 + W_{ij} & \text{if } W_{ij} \leq 0, \\ 1 - W_{ij} & \text{otherwise} \end{cases} \quad \forall i = 1 \dots I, j = 1 \dots J$
 - 6: Compute the weighted sum to all neurons for all input vectors
 $a^r = \frac{M}{2} (W^T \hat{x}^r + W^T \mathbf{1}) \quad \forall r = 1 \dots D$
 - 7: Constrain these weighted sums within their upper and lower limits
 $v_j^r \leq a_j^r \leq u_j^r \quad \forall r = 1 \dots D, j = 1 \dots J$
 - 8: **end procedure**
 - 9: **return** $t^r = \tanh(a^r) \quad \forall r = 1 \dots D$

far they are from 1 or -1 , whichever is closer. It effectively implements $W'_{ij} = \min(1 + W_{ij}, 1 - W_{ij})$; however this expression cannot be directly used as the minimum of affine functions is not convex [15]. This is also the reason why we impose a constraint on the range of the weights in line 4 (minimum of distance from 1 and -1 isn't convex). Line 6 computes the weighted sum inputs of the \tanh function, line 7 constrains them within the limits obtained in line 2, and line 9 finally returns the approximate neuron outputs. The optimization problem stated above is convex because the objective function and the inequality constraints are convex and the equality constraints are affine [15].

D. 2-layer NN

A similar formulation could have been made for NNs containing more than 1 layer, having the objective of minimizing the “sum of distances” of each of the weight matrices, with constraints computing the hidden layer(s) outputs and finally restricting the error in the output layer’s weighted sums. However, the presence of the non-convex activation function in the hidden layer(s) would make the problem (as a whole) non-convex. To mitigate this issue, we propose breaking down the problem into separate but identical convex problems, each of which optimizes the weights in successive layers of the NN under some error constraints. Thus, in a 2-layer NN having I inputs, L hidden neurons and J output neurons, we shall solve 2 problems successively - first for the hidden layer and then for the output layer, with error thresholds ϕ_Z and ϕ_W respectively. Notations used for the 2-layer network, for terms which do not appear in a 1-layer network, are described in Table III.

TABLE III: Notations for problem formulation of 2-layer NN

Name	Meaning	Type	Dimension
W, Z	The output and hidden layer weight matrix	Matrix	$L \times J, I \times L$
M_W, M_Z	The scaling factor of W and Z	Scalar	1
b^r	The r^{th} weighted sums of hidden neurons	Vector	L
h^r	The r^{th} hidden neuron outputs	Vector	L

1) Estimation of maximum tolerable ϕ_Z

In a 2-layer NN, given some value of ϕ_W , there exists an upper limit to the amount of error that can be tolerated at the outputs of the hidden layer. We know that the weighted sum input to the j^{th} neuron of the output layer is

$$a_j = \sum_{l=1}^L W_{lj} h_l \quad (11)$$

A constraint on the output layer outputs for all of the D inputs is written as

$$|\Delta t_j^r| = |t_j^r - \hat{t}_j^r| \leq \phi_W \quad \forall j = 1 \dots J, r = 1 \dots D \quad (12)$$

We use a first order approximation (from Taylor series expansion) to the errors in the weighted sums and write (12) as

$$|a_j^r - \hat{a}_j^r| \leq \frac{\phi_W}{f'(\hat{a}_j^r)} \quad \forall j = 1 \dots J, r = 1 \dots D \quad (13)$$

where f' is the first derivative of \tanh . Because \tanh is a monotonically increasing function, f' is always positive. To establish a lower bound, we need to consider the strictest of all constraints, which takes us to

$$|a_j - \hat{a}_j| \leq \min_r \left(\frac{\phi_W}{f'(\hat{a}_j^r)} \right) = \lambda_j \text{(say)} \quad \forall j = 1 \dots J \quad (14)$$

Because we are interested in deviations in hidden neuron outputs, using (11) and then writing $(h_l - \hat{h}_l) = y_l$, we obtain

$$\left| \sum_{l=1}^L W_{lj} (h_l - \hat{h}_l) \right| = \left| \sum_{l=1}^L W_{lj} y_l \right| \leq \lambda_j \quad \forall j = 1 \dots J \quad (15)$$

Algorithm 1 Problem Formulation for 2-layer NN

$$\begin{aligned} 1: h^r &= \text{OPTIMWEIGHTS}(I, L, \hat{Z}, \hat{x}, \hat{h}, M_Z, \phi_Z) & \forall r = 1 \dots D \\ 2: t^r &= \text{OPTIMWEIGHTS}(L, J, \hat{W}, h, \hat{t}, M_W, \phi_W) & \forall r = 1 \dots D \end{aligned}$$

The LHS of (15) represents a hyperplane (for each j) in the L -dimensional space, with slab constraint (15) having L variables and J equations.

Case 1: $L > J$. The feasible region defined by (15) is unbounded. Thus we can only estimate a lower bound on the maximum error tolerable at the hidden layer. The smallest y to violate the j^{th} constraint (say \tilde{y}_j) would be orthogonal to the j^{th} hyperplane and lying on it. Since each of the L hidden neurons must satisfy the error threshold, we shall consider the largest of the L coordinates of \tilde{y}_j for each of the J constraints. The lowest of J such values would provide a lower bound on the maximum acceptable error. Mathematically, lower bound

$$\bar{\phi}_Z = \min_j \left(\max_l |(\tilde{y}_j)_l| \right) \quad (16)$$

Because all equations are linear, $\bar{\phi}_Z$ can be obtained quickly through linear programming.

Case 2: $L \leq J$. The feasible region defined by inequality (15) is bounded. We can find a lower bound using the same argument as above, as well as an upper bound.

2) Problem Formulation

Algorithm 1 shows how the weights of the 2-layers can be optimized independently, with the output from the first being an input to the second. Recall that the error threshold ϕ_Z estimated in (16) provides only a lower bound to the maximum tolerable error. Thus, using this estimate may not yield the best approximation possible with the given ϕ_W and it is necessary to solve with higher values of the threshold ϕ_Z and look for better solutions (further approximations). We use a search-based method for this where we start with $\phi_Z = \bar{\phi}_Z$ and keep increasing ϕ_Z in steps as long as it's not large enough to make the optimization problem of the output layer (line 2 of Algo 1) infeasible, and then reduce it to within a desired accuracy.

V. EXPERIMENTAL METHODOLOGY AND RESULTS

Several benchmarks based on classification problems were used to measure the performance of the NNs and estimate the energy savings obtained by approximating the multiplications. First, we train an NN in MATLAB using the error back-propagation method, check its accuracy on the test dataset and estimate its power with the Normal MTJ-SNG. Next, we incorporate BMS (introduced in sec. III-C) and approximate the network using the optimization technique described in the previous section for different levels of error tolerance. For solving the optimization problems we use CVX, a package for specifying and solving convex programs [16]. Finally, each of the newly obtained NNs with approximate multipliers were analyzed for their accuracy and power.

The power consumption of the Normal MTJ-SNG and BMS in the networks were obtained from the data corresponding to the red and green (dotted) plots respectively in fig. 4(b) and those of the FSM-based \tanh from [8]. The results from the different datasets are summarized below:

MNIST digit recognition: The MNIST is a standard benchmark for classification problems that categorizes handwritten digits, each of size 28×28 [17]. First, a simple 1-layer NN with 784 inputs and 10 outputs was trained. This original network had an accuracy of 87.43% on the test dataset and power consumption of 707.9mW with the Normal MTJ-SNG. Table IV shows the benefit of replacing that with BMS. As can be seen from the 1st row, just the use of BMS reduces the power to

545.1mW, while maintaining the same accuracy. The following rows summarize the optimization results for different values of error tolerance. Significant energy savings were obtained even for $\phi_W = 0$ owing to certain degree of redundancy in some inputs. Classification accuracy drops by only 1.4% (with $\phi_W = 0.03$) for about 39% reduction in power when compared to the original, with 21% reduction over BMS (1st row) being achieved through optimization. We also observe how the classification accuracy, as well as the computation energy, vary with the precision of the stochastic streams.

TABLE IV: Variation of power with error, and of accuracy & energy with both error and precision for the MNIST 1-layer network with BMS. The *Inf* column corresponds to a theoretically infinite precision and the 1st row corresponds to BMS without any weight approximation.

ϕ_W	Power	Precision	Accuracy (in %)			Energy(μJ)		
			Inf	512	256	128	512	256
–	545.1 mW	87.43	87.41	87.59	81.97	2.18	1.09	0.54
0.00	443.8 mW	87.10	87.05	87.26	81.67	1.77	0.88	0.44
0.01	435.2 mW	86.74	86.79	86.59	83.51	1.74	0.87	0.43
0.02	431.4 mW	86.57	85.95	86.42	82.43	1.72	0.86	0.43
0.03	428.2 mW	86.03	86.17	85.82	84.29	1.71	0.85	0.42

For the 2-layer NN, input images were scaled down to size 14×14 to reduce the complexity of the problem (and hence the time required to solve it), and 15 neurons were used in the hidden layer. The original network had an accuracy of 92.28% and power of 273.68mW. Results of incorporating BMS and then approximating the network are shown in Table V, using ϕ_Z values that gave the least power. From the last column, it is evident that 43% decrement in power over the original, and 26% over BMS without approximation, was obtained with less than 1% degradation of accuracy.

TABLE V: MNIST 2-layer result. 1st column is BMS w/o approximation

ϕ_W	–	0.00	0.01	0.02	0.03	0.04	0.06	0.08
$\phi_Z(\times 10^{-2})$	–	0.00	0.64	1.28	1.92	2.56	2.88	3.84
Accuracy(in%)	92.28	92.18	92.14	92.07	92.02	91.97	91.72	91.35
Power(mW)	210.74	175.48	169.26	165.06	161.94	159.59	158.36	155.46

SONAR, Rocks vs. Mines: This dataset (as well as the next one) was obtained from the UCI Machine Learning Repository [18]. It requires us to distinguish between metal surfaces and rocks using sonar signals bounced off from them [19]. Both the training and test datasets contain 104 samples, each having 60 inputs. The accuracy and power of the original networks were 83 and 11.49mW respectively for the 1-layer NN, and 90 and 62.27mW for the 2-layer. Effect of using BMS and performance of our algorithm on both 1-layer NN and 2-layer NN (with 12 hidden neurons) are in Table VI. Unlike MNIST, here there was no power savings for $\phi_W = 0$. For the 1-layer NN, we observe 60% power reduction over original with accuracy degradation of 5 (for $\phi_W = 0.2$). For the 2-layer NN, the respective figures are 57% and 3 respectively.

TABLE VI: SONAR 1 and 2-layer. 1st column is BMS w/o approximation

1-layer NN	$\phi_W(\times 10^{-2})$	–	1	2	5	10	15	20
	Accuracy	83	83	83	82	81	81	78
2-layer NN	Power(mW)	8.85	7.71	7.18	6.48	5.66	4.96	4.62
	$\phi_Z(\times 10^{-2})$	–	0.675	1.48	3.9	7.8	14.625	18.2

Wine Quality: The goal is to train a network to estimate the quality of samples (on a scale of 10) of red and white wine on the basis of results of physiochemical tests [20]. Only 2-layer NNs with 20 hidden neurons were trained that gave accuracy of 86.4% and power 30.56mW with red wine, and 85.75% and 32.83mW respectively with white wine. Results are displayed in Table VII. Power savings over the original are 38% for accuracy

loss of 1.2% for Red wine, and 42% with loss in accuracy of 0.45% for White wine.

TABLE VII: Wine Quality - The 1st row is BMS without approximation

ϕ_W	ϕ_Z	Red Wine			White Wine		
		Accuracy	Power(mW)	$\phi_Z(\times 10^{-2})$	Accuracy	Power(mW)	
–	–	86.4%	23.53	–	85.75%	25.28	
0.02	0.021	86.4%	22.40	4.32	86.09%	22.39	
0.04	0.042	86.0%	21.36	2.16	85.86%	21.76	
0.10	0.042	86.4%	20.14	2.16	86.86%	20.46	
0.15	0.056	85.6%	19.30	6.48	85.97%	19.79	
0.20	0.070	85.2%	18.89	2.16	85.30%	19.19	

VI. CONCLUSION

This paper proposes the use of MTJs as SNGs in an SC based hardware implementation of Neural Networks. We design a low-power version of an MTJ-SNG (named BMS) that significantly reduces the average energy per bit of a stochastic stream and propose its use in an SC-based NN. We go on to develop an algorithm based on convex optimization that adjusts the weights in such an NN by leveraging the error resilient nature of applications of NNs. Classification problems were evaluated on this approximate NN and results showed substantial gains in energy savings for little loss in accuracy.

VII. ACKNOWLEDGEMENT

This work is supported by the Air Force Office of Scientific Research under Grant FA9550-14-1-0351.

REFERENCES

- [1] S. Samarasinghe, *Neural networks for applied sciences and engineering: from fundamentals to complex pattern recognition*. CRC Press, 2016.
- [2] S. Venkataramani *et al.*, “Axnn:energy-efficient neuromorphic systems using approximate computing,” in *ISLPED’14*. ACM, 2014, pp. 27–32.
- [3] V. Mrazek *et al.*, “Design of power-efficient approximate multipliers for approximate artificial neural networks,” in *ICCAD (prijato)*, 2016, p. 7.
- [4] J. Han *et al.*, “Approximate computing: An emerging paradigm for energy-efficient design,” in *18th IEEE ETS*, 2013, pp. 1–6.
- [5] A. Alaghi *et al.*, “Survey of stochastic computing,” *ACM Transactions on Embedded computing systems (TECS)*, vol. 12, no. 2s, p. 92, 2013.
- [6] J. Kim *et al.*, “A technology-agnostic mtj spice model with user-defined dimensions for stt-mram scalability studies,” in *Custom Integrated Circuits Conference (CICC)*, IEEE, 2015, pp. 1–4.
- [7] L. A. de Barros Naviner *et al.*, “Stochastic computation with spin torque transfer magnetic tunnel junction,” in *IEEE NEWCAST’15*, 2015, pp. 1–4.
- [8] A. Ardakani *et al.*, “VLSI implementation of deep neural networks using integral stochastic computing,” in *9th ISTC*. IEEE, 2016, pp. 216–220.
- [9] Q. Zhang *et al.*, “Approxann: an approximate computing framework for artificial neural network,” in *DATE*. EDA Cons., 2015, pp. 701–706.
- [10] M. Tarkov, “Mapping weight matrix of a neural networks layer onto memristor crossbar,” *Optical Memory and Neural Networks*, vol. 24, no. 2, pp. 109–115, 2015.
- [11] M. Hu *et al.*, “Dot-product engine for neuromorphic computing: programming 1T1M crossbar to accelerate matrix-vector multiplication,” in *53rd Design Automation Conference (DAC)*. IEEE, 2016, pp. 1–6.
- [12] K. Kim *et al.*, “Dynamic energy-accuracy trade-off using stochastic computing in deep neural networks,” in *DAC’16*. ACM, 2016, p. 124.
- [13] R. Venkatesan *et al.*, “Spintastic: spin-based stochastic logic for energy-efficient computing,” in *DATE’15*. IEEE, 2015, pp. 1575–1578.
- [14] Z. Diao *et al.*, “Spin-transfer torque switching in magnetic tunnel junctions and spin-transfer torque random access memory,” *Journal of Physics: Condensed Matter*, vol. 19, no. 16, p. 165209, 2007.
- [15] S. Boyd *et al.*, *Convex optimization*. Cambridge university press, 2004.
- [16] M. Grant *et al.*, “CVX: Matlab software for disciplined convex programming, version 2.1,” <http://cvxr.com/cvx>, Mar. 2014.
- [17] Y. LeCun *et al.*, “The mnist database of handwritten digits,” 1998. [Online]. Available: <http://yann.lecun.com/exdb/mnist>
- [18] M. Lichman, “UCI machine learning repository,” 2013. [Online]. Available: <http://archive.ics.uci.edu/ml>
- [19] R. P. Gorman *et al.*, “Analysis of hidden units in a layered network trained to classify sonar targets,” *Neural Networks*, vol. 1, p. 75, 1988.
- [20] P. Cortez *et al.*, “Modeling wine preferences by data mining from physicochemical properties,” *Decision Support Systems*, vol. 47, no. 4, pp. 547 – 553, 2009. [Online]. Available: <http://www.sciencedirect.com/science/article/pii/S0167923609001377>